Waveform analysis of the 1999 Hector Mine foreshock sequence

Eva E. Zanzerkia and Gregory C. Beroza
Department of Geophysics, Stanford University, Stanford, CA, USA

John E. Vidale
Department of Earth and Space Sciences, UCLA, Los Angeles, CA, USA

Received 2 October 2002; revised 5 December 2002; accepted 6 February 2003; published 23 April 2003.

[1] By inspecting continuous Trinet waveform data, we find 42 foreshocks in the 20-hour period preceding the 1999 Hector Mine earthquake, a substantial increase from the 18 foreshocks in the catalog. We apply waveform cross-correlation and the double-difference method to locate these events. Despite low signal-to-noise ratio data for many of the uncataloged foreshocks, correlation-based arrival time measurements are sufficient to locate all but three of these events, with location uncertainties from ~100 m to 2 km. We find that the foreshocks fall on a different plane than the initial subevent of the mainshock, and that the foreshocks spread out over the plane with time during the sequence as the time of the mainshock approaches. *INDEX TERMS:* 7230 Seismology: Seismicity and seismotectonics; 7294 Seismology: Instruments and techniques; 7299 Seismology: General or miscellaneous. **Citation:** Zanzerkia, E. E., G. C. Beroza, and J. E. Vidale, Waveform analysis of the 1999 Hector Mine foreshock sequence, *Geophys. Res. Lett.*, *30*(8), 1429, doi:10.1029/2002GL016383, 2003.

1. Introduction

[2] Foreshocks provide the clearest indication of precursory activity before at least some earthquakes [*Jones and Molnar*, 1979]. For this reason, it is important to understand as much as we can about the mechanics and statistics of foreshock sequences. Nearly half of all well-recorded earthquakes have at least one foreshock [*Jones* 1984; *Abercrombie and Mori*, 1996].

[3] The M7.1, October 16, 1999 Hector Mine earthquake, shown in Figure 1, is documented to have been preceded by a sequence of 18 foreshocks in the 20 hours before the mainshock [*Hauksson et al.*, 2002]. These foreshocks were detected and located by the Southern California Seismic Network (SCSN). We have examined the same period by eye using continuous waveforms from the stations nearest to the foreshock sequence and have found at least 42 foreshocks in the sequence over this time period. Standard event detection algorithms must be conservative in order to avoid many false alarms. However, this difference between the cataloged foreshocks and the additional events suggests that we may be able to learn a great deal more by studying continuous data during sequences of special interest. The fact that so many of the Hector Mine foreshocks went uncataloged also suggests that foreshocks may be more common than previously reported.

0094-8276/03/2002GL016383$05.00

[4] Although the Hector Mine foreshock sequence occurred in an area of sparse instrumentation, we are able to obtain precise locations for 39 of the 42 foreshocks by making precise arrival time measurements from waveform data even at low signal to noise ratio (*snr*) and double-difference relocation. After relocation we find that the foreshocks occurred on the mainshock initiation plane and that the extent of the foreshock zone expands as the time of the mainshock approaches.

2. Event Identification

[5] Initially, 18 foreshocks were identified by the SCSN in the 20 hours preceding the Hector Mine earthquake. These events were recorded by the TriNet/SCSN network, which is divided into 75 overlapping subnets. The network detection protocol has several stages. If four or more stations in a subnet detected a signal strength that is greater than the noise, then a trigger is identified for that subnet. An identified event is then reviewed by a seismic analyst for phase picking. The foreshocks to the Hector Mine earthquake range in magnitude from M 1.3 to 3.7, and are clustered in two temporal clusters. Although the network is sparse in this area of California, these events are sufficiently prominent at enough stations to catalog and obtain reasonable locations.

[6] There are, however, other foreshocks in this time period that are not cataloged or located. In the continuous records at the six stations closest to the Hector Mine mainshock, we found an additional 24 foreshocks that were not previously cataloged. Moreover, three additional events with similar waveforms can be identified only at CDY, the closest station to the foreshocks. This brings the number of foreshocks visible in this sequence to 45, using this method. The first 25 events occur 20–13 hours before the mainshock, and the next 17 begin five hours after that, with the latest occurring just 19 minutes before the mainshock, as shown in Figure 2b.

[7] CDY shows the clearest record of the foreshocks (Figure 2a). Many of the smaller and uncataloged waveforms have low *snr*. Also, two events with clearly discernable phases show opposite polarity from the other events. This may mean that these events have a different focal mechanism from the other events and suggests the involvement of more than one fault plane at the mainshock initiation point.

[8] The other stations used to relocate the uncataloged events (CPM, GTM, RMM, RMR and TPC) are also shown in Figure 1. All of the cataloged foreshocks and a few of the uncataloged foreshocks are also detectable at GRP, the sole station nearly due east of the foreshock sequence; however, most of the uncataloged foreshocks are poorly recorded there

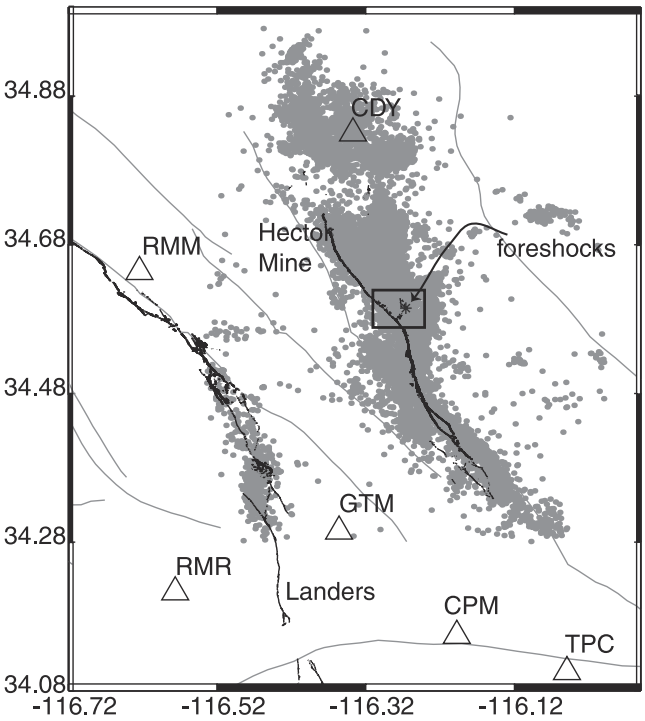

Figure 1. The Hector Mine surface rupture shown in black, aftershocks in gray. Triangles denote the six SCSN stations where all 42 foreshocks were recorded.

because the *snr* is too low for such small events. This means that the station coverage is highly non-uniform, with large gaps particularly to the east of the sequence and is especially severe for some of the uncataloged events. Although this station coverage is not ideal for relocation, there is still enough data to recover good locations for both the cataloged and uncataloged foreshocks, particularly if we can measure *S*-wave arrival times as well as *P*-wave arrival times.

3. Data Analysis

3.1. Correlation

[9] We located the foreshocks using waveform cross-correlation [*Schaff et al.*, 2002b] and double difference relocation [*Waldhauser and Ellsworth*, 2000]. We use a time domain method that Schaff et al. have shown to be a robust method for obtaining relative arrival times, but use both time and frequency domain correlation techniques to define the quality of the data that we keep [*Schaff et al.*, 2003]. We perform the cross correlation over a window centered on a preliminary phase pick, using a 128-sample window and a 0.01-sec sampling rate. For waveforms at CDY, the phase arrivals are handpicked, while at the other five stations, the arrivals are estimated relative to the arrival at CDY and visually reviewed.

[10] In datasets of repeating or closely spaced events on the Calaveras fault, *Schaff et al.* [2002a] used arrival time measurements with correlation coefficients greater than 60% because these observations were found to provide precise data, based on their low post-fit residuals, for relocation. In this study we also use a correlation coefficient of 60% as the cutoff for observations involving uncataloged events. For cataloged events, the number of observations is large enough to allow using only data with a somewhat higher correlation coefficient cutoff of 70%. This higher threshold reduces the possibility of introducing outliers.

[11] For cataloged foreshocks, we supplement the data from the six closest stations with relative arrival time measurements from approximately 190 other stations in the network where these events were measured. Unfortunately, this additional information is not available for the uncataloged events, because these events were too small or noisy to be detected at those stations. This means that during relocation these events may not have enough observations to find a well-constrained solution, and may be more strongly influenced by the asymmetric station geometry or outliers, increasing their location error.

4. Relocations

[12] We compiled a dataset of 4111 *P*-wave and 3817 *S*-wave relative arrival times, through waveform cross-correlation. The double-difference relocation method allows us to use relative arrival time information and reduces location error due to unmodeled velocity variations [*Waldhauser and Ellsworth*, 2000]. We use the velocity model from *Wald et al.* [1995].

[13] It is difficult to obtain accurate relative arrival times between a large magnitude event, like the mainshock, and small foreshocks, using cross correlation because of waveform clipping and differences in spectral content. In order to calculate a more precise location for the mainshock, we use a reference foreshock with a clear first break to assign first break times to foreshocks that correlate with the reference event. These first break times are then differenced with the

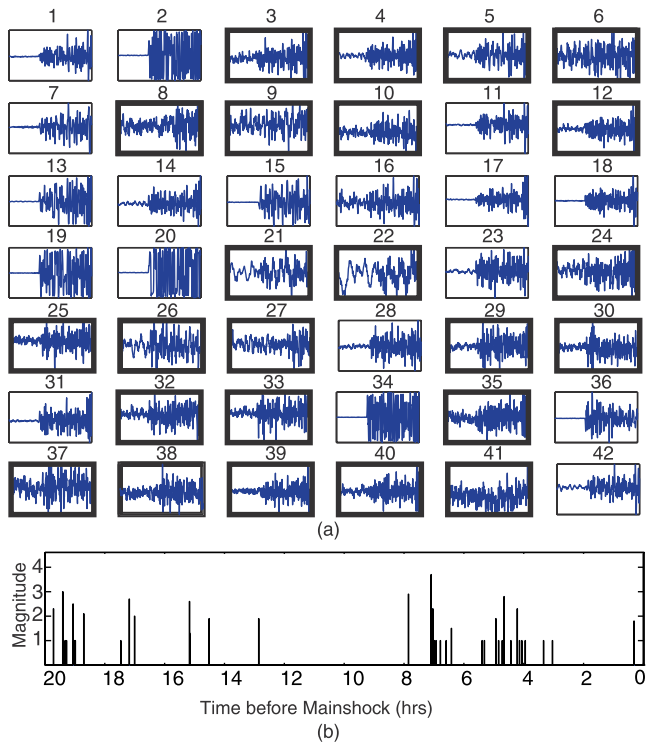

Figure 2. (a) Seismograms showing 6 sec around the P-arrival time for the 42 foreshocks at CDY. Events are in chronological order; events with bold outlines for previously uncataloged foreshocks. (b) Foreshock magnitude over time in hours before mainshock.

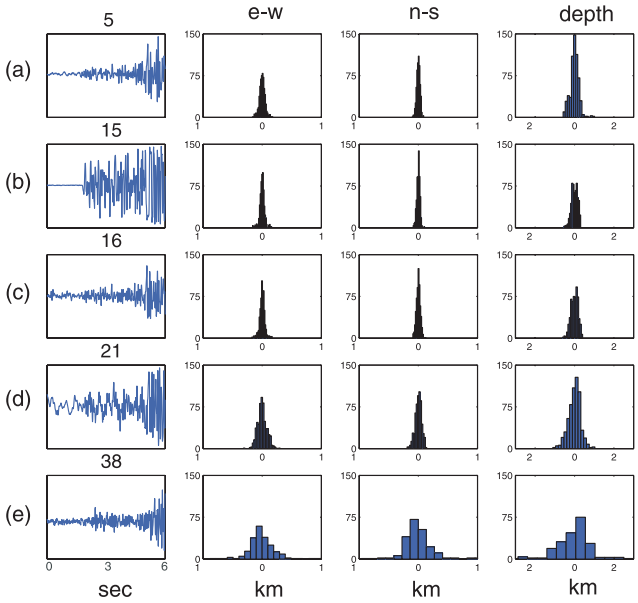

Figure 3. Waveforms, 6 sec around the *P*-wave arrival, for selected foreshocks, with histograms of the x, y, and depth distributions, in kilometers, of the bootstrapped locations. Events 5, 21 and 38, represented by rows (a), (d) and (e), respectively, are previously uncataloged foreshocks.

mainshock arrival time to give us relative arrival times for the mainshock.

[14] We first relocate all the events using all the data, which results in locations for 40 events, including the mainshock. Initially, we assign the uncataloged events a starting location that is the mean location of all the foreshocks because the uncataloged events do not have initial locations. During the relocation, data is culled through residual reweighting and parameters derived from the relocation, such as the distance between event pairs. This leads to the elimination of 25% of the data and three events. The three events were all uncataloged foreshocks with very low *snr*.

[15] Next, we used a bootstrap of the post-fit residuals to estimate the relative location error of the events [*Efron*, 1982; *Waldhauser and Ellsworth*, 2000]. Waldhauser et al. used a bootstrap for double-difference locations, as well, to constrain the error in a set of repeating events and found the errors to be accurately represented. Our situation is quite different. Instead of repeating earthquakes, we have separate events of varying magnitude, location, and with a sparse and uneven station distribution. The data quality in our sequence may stretch the assumption of normally distributed errors.

[16] We start the bootstrap by adding randomly sampled residuals, with replacement, to relative arrival times calculated from our locations, and this new data is used in the relocation code to obtain new locations. This procedure is repeated 600 times, and the locations from all iterations are saved. We may only perform the bootstrap on events that were initially relocated (40 events including the mainshock). The final locations are taken as the mean of all locations from the iterations. We also calculate 95% confidence intervals for each foreshock location. These represent relative location errors, since we removed the mean location from each iteration.

[17] Our relocations are much more precise than the catalog locations, which for this region have errors on the order of 1 to 2 km. Most events, as shown by the examples in Figure 3, have errors on the order of ±60–150 m horizontally, and ±200–300 m vertically. A few events have errors of 1–2 km. The errors obtained from the bootstrap are anywhere from 5 to 30 times greater than the formal errors calculated during the relocation. The bootstrap and formal errors in the horizontal are not well correlated; events with large bootstrap errors do not necessarily have large formal errors.

[18] Figures 3b and 3c show cataloged foreshocks, with event 16 exhibiting an *snr* similar to that of many of the uncataloged events, like event 5 (Figure 3a). Despite the greater station coverage for event 16, both events have comparable errors. An event with a clear phase arrival does not necessarily fare significantly better, showing similar location variability to other events. However, foreshocks with low *snr* show a greater variability in location; event 38 shown in Figure 3e, has errors on the order of 500 m

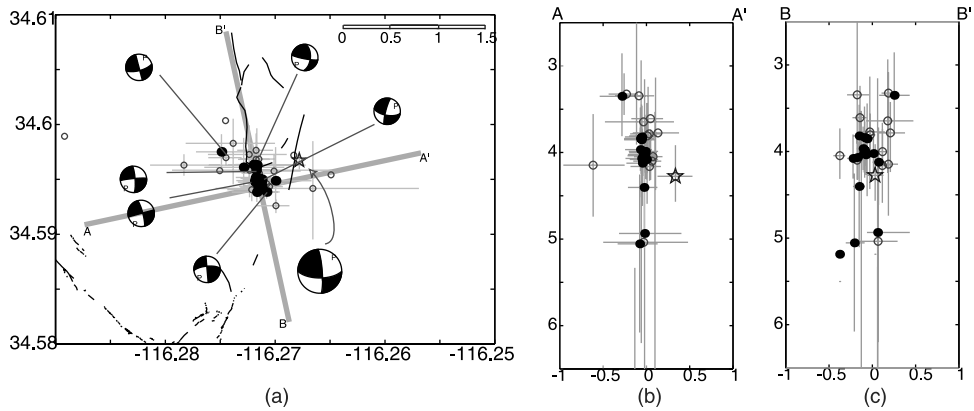

Figure 4. (a) Map view of locations with 95% confidence error bars less than 1.5 kms. Filled circles are events occurring between 20 and 13 hrs prior to the mainshock, and open circles are foreshocks occurring 8 to 0 hrs before the mainshock. The star represents the relocated mainshock hypocenter, and the focal mechanisms [*Hauksson et al.*, 2002] correspond the mainshock and the six largest foreshocks. (b) A-A′ cross-section with 95% confidence error bars. (c) B-B′ cross-section with error bars. In the cross-section plots, only events with horizontal errors less than 400 m are shown.

horizontally and 1–2 km in depth. All events show a greater longitudinal error than latitudinal error, which is attributable to the gap in coverage to the east. As expected, the cataloged foreshocks all have low errors, while the uncataloged foreshocks have a wider range of errors, from 100 m to 2 km.

5. Foreshock Analysis

[19] After relocation, most of the 39 foreshocks (Figure 4) are compactly clustered in a 1 km by 1 km region and most are near a plane extending ~0.75 km in a N12°W direction and vertically in depth. This corresponds with the N-NW trending surface expression of the mainshock rupture near where the mainshock itself initiated [*Hauksson*, 2002]. The foreshocks range in depth from 3 to 6 km, with most events clustering at 3.5 to 4.5 km. These events have smaller vertical errors than those at greater depths.

[20] Mechanisms available for six foreshocks are consistent with these locations, as well as with the mainshock's mechanism [*Hauksson*, 2002]. The relocation of the mainshock, shown by the star in Figure 4a, is on a different plane from foreshocks. However, the 95% confidence error bars of the mainshock overlap those of a few of the foreshocks in the well-defined plane. By performing a bootstrap test on the best-fitting plane to the foreshocks and comparing the results to the mainshock's position, we may exclude the mainshock from the plane of the foreshocks at a 95% confidence. There are other foreshock sequences that similarly have been displaced from their mainshocks [*Dodge et al*., 1996; *Jones et al.*, 1982].

[21] We also observe that the foreshocks occur in two distinct time periods that exhibit different spatial patterns. 20 to 13 hours before the mainshock, the foreshocks fall almost exclusively on a well-defined plane (black circles in Figure 4). There is a five-hour gap between this activity and the cluster occurring from eight to three hours prior to the mainshock (open circles in Figure 4). After a M2.0 and a M3.7 foreshock that occur about eight hours prior to the mainshock, the subsequent foreshocks are more diffuse. Location error on some of these later events, however, makes it difficult to determine how much of this expansion is real. Also, there is no clear, sequential progression of foreshocks towards the mainshock, or indication that prior events are directly triggering subsequent events.

[22] Other investigators have examined expanding foreshock zones as a potential indication of nucleation zone size [*Ohnaka*, 1992; *Abercrombie et al*, 1995; *Dodge et al*, 1996]. Dodge et al. find that foreshock hypocenters for the six sequences they studied tended towards the mainshock hypocenter over time more than they expand away from their own centroid.

[23] Although there is slightly more spread in location of the later Hector Mine foreshocks than the earlier ones, there is no dramatic expansion away from the foreshock centroid. Unfortunately, this measurement is dominated by the depth variation. If we look only at distance from the mainshock in two dimensions, we find that some later foreshocks fall closer to the mainshock hypocenter than most of the earlier foreshocks, which suggests slip localization as described for faults modeled with rate- and state-dependent strength [*Dieterich*, 1992]. We note that the size of the Hector Mine nucleation zone is consistent with a possible scaling of foreshock zone extent with earthquake magnitude found by *Dodge et al.* [1996], and qualitatively, the lack of triggering in the foreshock sequence, the foreshock mechanisms and the mainshock location in the stress shadow of the foreshocks do not suggest static stress triggering.

6. Conclusions

[24] From a visual examination of the continuous record, we find that the Hector Mine foreshock sequence contains at least 45 events, not just 18 as originally identified from locations in the SCSN. It appears that foreshocks may be more common than previously thought. The sequence delineated a clear N-NW trending structure, and seems to occurs on a different plane from the mainshock initiation. Low *snr* doesn't necessarily prevent reliable relative arrival time information from cross-correlation, opening up more and diverse regions of seismicity for correlation and relocation.

[25] **Acknowledgments.** We thank Norm Sleep for the mainshock correlation method, and Mariagiovanna Guatteri for bootstrap work. This research was supported by the Southern California Earthquake Center. SCEC is funded by NSF Cooperative Agreement EAR-8920136 and USGS Cooperative Agreements 14-08-0001-A0899 and 1434-HQ-97G01718. The SCEC contribution number for this paper is 707.

References

Abercrombie, R. E., D. C. Agnew, and F. K. Wyatt, Testing a model of earthquake nucleation, *Bull. Seismol. Soc. Am.*, *85*, 1873–1878, 1995.

Abercrombie, R. E., and J. Mori, Occurrence patterns of foreshocks to large earthquakes in the western United States, *Nature*, *381*, 303–307, 1996.

Dieterich, J. H., Earthquake nucleation on faults with rate- and state-dependent strength, *Tectonophysics*, *211*, 115–134, 1992.

Dodge, D. A., G. C. Beroza, and W. L. Ellsworth, Detailed observations of California foreshock Sequences: implications for the earthquake initiation process, *J. Geophys. Res.*, *101*, 22,371–22,392, 1996.

Efron, B., The jackknife, the bootstrap, and other resampling plan, SIAM, 92 pp., 1982.

Hauksson, E., L. M. Jones, and K. Hutton, The 1999 Mw7.1 Hector Mine, California Earthquake Sequence: Complex Conjugate Strike-Slip Faulting, *Bull. Seismol. Soc. Am.*, *92*, 1154–1170, 2002.

Jones, L. M., Foreshocks (1966–1980) in the San Andreas Fault system, California, *Bull. Seismol. Soc. Am.*, *74*, 1361–1380, 1984.

Jones, L. M., and P. Molnar, Some characteristics of foreshocks and their possible relationship to earthquake prediction and premonitory slip on faults, *J. Geophys. Res.*, *84*, 3596–3608, 1979.

Jones, L. M., B. Wang, S. Xu, and T. Fitch, The foreshock sequence of the February 4, 1975 Haicheng earthquake (M = 7.3), *J. Geophys. Res.*, *87*, 4575–4584, 1982.

Ohnaka, M., Earthquake source nucleation: A physical model for short term precursors, *Tectonophysics*, *211*, 149–178, 1992.

Schaff, D. P., G. H. R. Bokelmann, G. C. Beroza, F. Waldhauser, and W. L. Ellsworth, High Resolution Image of Calaveras Fault Seismicity, *J. Geophys. Res.*, *107*, 633, 2002a.

Schaff, D. P., G. H. R. Bokelmann, E. Zanzerkia, F. Waldhauser, G. C. Beroza, and W. L. Ellsworth, Cross correlation arrival time measurements for earthquake location, submitted, BSSA, 2003.

Wald, D. J., L. K. Hutton, and D. D. Given, The Southern California Network Bulletin: 1990–1993 summary, *Seismol. Res. Lett.*, *66*, 9–19, 1995.

Waldhauser, F., and W. L. Ellsworth, A double-difference earthquake location algorithm: method and application to the northern Hayward Fault, California, *Bull. Seismol. Soc. Am.*, *90*, 1353–1368, 2000.

E. E. Zanzerkia and G. C. Beroza, Department of Geophysics, 397 Panama Mall, Stanford University, Stanford, CA 94305-2215, USA.

J. E. Vidale, Department of Earth and Space Sciences, UCLA, 595 Charles Young Drive East,Box 951567, Los Angeles, CA 90095-1567, USA.